

RIS-Assisted Code-Domain MIMO-NOMA

Bashar Tahir, Stefan Schwarz, and Markus Rupp

Institute of Telecommunications, Technische Universität Wien, Vienna, Austria

Abstract—We consider the combination of uplink code-domain non-orthogonal multiple access (NOMA) with massive multiple-input multiple-output (MIMO) and reconfigurable intelligent surfaces (RISs). We assume a setup in which the base station (BS) is capable of forming beams towards the RISs under line-of-sight conditions, and where each RIS is covering a cluster of users. In order to support multi-user transmissions within a cluster, code-domain NOMA via spreading is utilized. We investigate the optimization of the RIS phase-shifts such that a large number of users is supported. As it turns out, it is a coupled optimization problem that depends on the detection order under interference cancellation and the applied filtering at the BS. We propose to decouple those variables by using sum-rate optimized phase-shifts as the initial solution, allowing us to obtain a decoupled estimate of those variables. Then, in order to determine the final phase-shifts, the problem is relaxed into a semidefinite program that can be solved efficiently via convex optimization algorithms. Simulation results show the effectiveness of our approach in improving the detectability of the users.

I. INTRODUCTION

Reconfigurable intelligent surfaces (RISs) have emerged as a promising technology for beyond fifth-generation (B5G) wireless communication, enabling operation with high spectral and energy efficiency [1], [2]. Consisting of configurable nearly-passive elements, those surfaces are capable of altering the propagation of the electromagnetic waves impinged on them, allowing them to perform passive beamforming of the waves from and to a certain point, suppress interference, extend the coverage area, etc [3], [4]. Combining RISs with non-orthogonal multiple access (NOMA) has been the focus of many works, such as [5]–[9], showing potential gains in terms of the energy efficiency, sum-rate, and outage performance. In NOMA, multiple user equipments (UEs) occupy the same time-frequency resources, which may lead to a higher spectral efficiency, lower access latency, improved user fairness [10], [11]. So far, those works focused on pure power-domain NOMA, and on the optimization of the RIS phase-shifts under NOMA interference cancellation (IC). Little attention has been given to code-domain NOMA, where on top of the power-domain superposition, the UEs transmit with code-domain signatures (e.g., short spreading sequences), which permits interference suppression at the receiver via code-domain processing [12], [13]. Such an interference suppression capability allows for a large number of simultaneous transmissions; combined with massive multiple-input multiple-output (MIMO), this can help enabling massive connectivity.

Bashar Tahir and Stefan Schwarz are with the Christian Doppler Laboratory for Dependable Wireless Connectivity for the Society in Motion. The financial support by the Austrian Federal Ministry for Digital and Economic Affairs and the National Foundation for Research, Technology and Development is gratefully acknowledged.

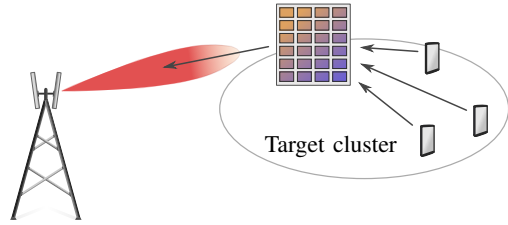


Fig. 1: The cluster-based RIS-assisted NOMA uplink.

We investigate here the combination of uplink code-domain NOMA with RISs, in the context of a cluster-based massive MIMO deployment. Since it is likely that those surfaces would be deployed at rooftops, we make the assumption that each cluster is served by a RIS having a strong line-of-sight (LOS) connection to the base station (BS). The BS forms beams towards the clusters' RISs, allowing to simultaneously boost the received power of the target cluster and suppress intercluster interference, as depicted in Figure 1. In order to support massive connectivity, code-domain NOMA via short spreading is employed in each cluster. At the BS, and after spatial filtering, minimum mean square error (MMSE)-IC detection is carried out to detect the NOMA UEs. The question then is, how to configure the RIS such that a large number of UEs is supported? As we will see later, it is a coupled optimization problem that depends on multiple variables, such as the detection order under IC, and the applied MMSE filters. To this end, we propose to obtain a decoupled estimate of those variables by utilizing sum-rate optimized phase-shifts as an initial solution. We then find the final shifts by a semidefinite programming (SDP) relaxation of the optimization problem, which can be solved efficiently via the framework of convex optimization. The simulation results show that our proposed approach can substantially improve the detection performance.

II. SYSTEM MODEL

We consider a cluster of K single-antenna UEs communicating with an N_r -antennas BS through an N_s -elements RIS. Due to blockage, we assume the communication to take place primarily through the RIS, and therefore we drop the direct paths between the UEs and the BS. We will further justify this assumption later. Each UE transmits using a short spreading signature of length L , assigned to them by the BS based on a non-orthogonal spreading codebook. Assuming the channel is flat over the spreading interval (valid for small L), the received signal at the BS, $\mathbf{y} \in \mathbb{C}^{N_r L \times 1}$, is given by

$$\mathbf{y} = \sum_{k=1}^K \sqrt{\ell_{\text{BS}} \ell_{h_k} P_k L} (\mathbf{H}_{\text{BS}} \Phi \mathbf{h}_k \otimes \mathbf{s}_k) x_k + \mathbf{z} + \mathbf{n}, \quad (1)$$

where ℓ_{BS} and ℓ_{h_k} are the pathlosses of the BS-RIS and k^{th} RIS-UE channels, respectively, and P_k is the transmit power of the k^{th} UE. The quantities $\mathbf{H}_{\text{BS}} \in \mathbb{C}^{N_r \times N_s}$ and $\mathbf{h}_k \in \mathbb{C}^{N_s \times 1}$ represent the small-scale fading of the BS-RIS and k^{th} RIS-UE channels, respectively. The matrix $\Phi \in \mathbb{C}^{N_s \times N_s} = \text{diag}(e^{j\phi_1}, e^{j\phi_2}, \dots, e^{j\phi_{N_s}})$ is the phase-shift matrix applied at the RIS, where ϕ_n is the phase-shift applied at the n^{th} element. The operator \otimes denotes the Kronecker product, $\mathbf{s}_k \in \mathbb{C}^{L \times 1}$ is the unit-norm spreading signature, and x_k is the transmitted symbol. The term $\mathbf{z} \in \mathbb{C}^{N_r L \times 1}$ is the sum of all received signals from outside the intended cluster, i.e., intercluster interference, and $\mathbf{n} \in \mathbb{C}^{N_r L \times 1}$ is the zero-mean complex Gaussian noise with variance $\sigma_{\mathbf{n}}^2$. The description using the Kronecker product follows from the fact that at each BS antenna, a spreading block (e.g., over neighbouring subcarriers) of length L is received, and therefore the total received signal (over space and frequency) is of size $N_r L$. This, combined with the assumption of the channel being flat over the spreading block, allows for this compact description. Since the RIS is deployed in a LOS to the BS, the BS-RIS channel is rank-1, and is given by $\mathbf{H}_{\text{BS}} = \mathbf{a}\mathbf{b}^H$, where \mathbf{a} and \mathbf{b} are the array responses at the BS and RIS, respectively. The received signal can then be written as

$$\mathbf{y} = (\mathbf{a} \otimes \mathbf{I}_L) \sum_{k=1}^K \sqrt{\ell_{\text{BS}} \ell_{h_k} P_k L} (\mathbf{b}^H \Phi \mathbf{h}_k \otimes \mathbf{s}_k) x_k + \mathbf{z} + \mathbf{n}, \quad (2)$$

where \mathbf{I}_L is the identity matrix of size L . Equipped with a large number of antennas, the BS forms a beam towards the cluster's RIS, boosting the received power on the one hand, and on the other hand, suppressing intercluster interference. To achieve that, beam forming via maximum-ratio combining (MRC) is performed. This further justifies the assumption of dropping the direct path between the UEs and the BS, as it would be even weaker after beamforming. The MRC spatially filtered signal $\tilde{\mathbf{y}} = (\mathbf{a}^H \otimes \mathbf{I}_L) \mathbf{y}$ is given by

$$\begin{aligned} \tilde{\mathbf{y}} &= (\mathbf{a}^H \mathbf{a} \otimes \mathbf{I}_L) \sum_{k=1}^K \sqrt{\ell_{\text{BS}} \ell_{h_k} P_k L} (\mathbf{b}^H \Phi \mathbf{h}_k \otimes \mathbf{s}_k) x_k \\ &\quad + (\mathbf{a}^H \otimes \mathbf{I}_L) \mathbf{z} + (\mathbf{a}^H \otimes \mathbf{I}_L) \mathbf{n}. \end{aligned} \quad (3)$$

With the beamforming towards the target RIS, intercluster interference is greatly reduced, i.e., $(\mathbf{a}^H \otimes \mathbf{I}_L) \mathbf{z} \approx \mathbf{0}$. Since we have $\mathbf{a}^H \mathbf{a} = N_r$, and letting $\tilde{\mathbf{n}} = (\mathbf{a}^H \otimes \mathbf{I}_L) \mathbf{n}$ be the spatially filtered noise with $\sigma_{\tilde{\mathbf{n}}}^2 = N_r \sigma_{\mathbf{n}}^2$, (3) is further developed as

$$\tilde{\mathbf{y}} = \sum_{k=1}^K \sqrt{N_r^2 \ell_{\text{BS}} \ell_{h_k} P_k L} (\mathbf{b}^H \Phi \mathbf{h}_k \otimes \mathbf{s}_k) x_k + \tilde{\mathbf{n}}. \quad (4)$$

Notice that $\mathbf{b}^H \Phi \mathbf{h}_k$ is a scalar and therefore \otimes is no longer necessary. Let $\beta_k = \sqrt{N_r^2 \ell_{\text{BS}} \ell_{h_k} P_k L}$, $\mathbf{w} = \text{diag}(\Phi^H)$, and $\hat{\mathbf{h}}_k = \mathbf{b}^* \circ \mathbf{h}_k$, where \circ denotes the Hadamard product, the post-spatially filtered signal can finally be written as

$$\tilde{\mathbf{y}} = \sum_{k=1}^K \beta_k (\mathbf{w}^H \hat{\mathbf{h}}_k) \mathbf{s}_k x_k + \tilde{\mathbf{n}}. \quad (5)$$

In order to detect the UEs within the cluster, the BS performs MMSE-IC detection, with a UE being detected correctly if its signal-to-interference-plus-noise ratio (SINR) exceeds a certain rate threshold. Assuming a successive IC in which one UE is detected per IC stage, and assuming a detection order of UE 1, UE 2, \dots , UE K , the post-filtering SINR of the k^{th} UE is given by

$$\text{SINR}_k = \frac{|\beta_k (\mathbf{w}^H \hat{\mathbf{h}}_k) \mathbf{v}_k^H \mathbf{s}_k|^2}{\sum_{l=k+1}^K |\beta_l (\mathbf{w}^H \hat{\mathbf{h}}_l) \mathbf{v}_k^H \mathbf{s}_l|^2 + \sigma_{\tilde{\mathbf{n}}}^2 \|\mathbf{v}_k\|^2}, \quad (6)$$

where \mathbf{v}_k is the MMSE filter applied at the k^{th} stage. As can be seen, every time a UE is removed, the next UE in the next IC stage experiences less interference, until we reach the last UE, in which it only has to deal with noise. The goal now is to design \mathbf{w} such that

$$\text{SINR}_k \geq \epsilon_k, \quad \forall k, k = 1, 2, \dots, K, \quad (7)$$

where ϵ_k is the detection threshold of the k^{th} UE. In other words, we choose the phase-shifts at the RIS such that the power gaps between the UEs combined with the MMSE filtering and IC result in SINRs exceeding the required threshold for decodability, at each of the IC stages.

We have multiple problems here; first, the detection order of the UEs, to begin with, is unknown and it depends on the choice of \mathbf{w} . This can be clearly seen in (5), where the received power of the users is directly impacted by the choice of \mathbf{w} . In other words, the optimal detection order and \mathbf{w} need to be determined jointly, requiring a search over all possible detection orders, which can be of prohibitive complexity for large K ; second, the resulting SINR at each stage depends on the MMSE filter \mathbf{v}_k ; however, \mathbf{v}_k also depends on \mathbf{w} and the detection order (coupled), and therefore determining \mathbf{w} depends on the resulting \mathbf{v}_k ; third, even if everything is known, how do we find a \mathbf{w} satisfying all of the K inequalities in (7)?

III. SUM-RATE OPTIMIZED PHASE-SHIFTS

It is known from the MIMO literature that MMSE-IC is a sum-rate optimal detection scheme [14]. Therefore, one way to avoid the aforementioned problems with the detection order and the choice of the MMSE filter, is to optimize \mathbf{w} such that the sum-rate of the cluster is maximized. To that end, the sum-rate is given by

$$R_{\text{sum}} = \frac{1}{L} \log_2 \det \left(\mathbf{I}_L + \frac{1}{\sigma_{\tilde{\mathbf{n}}}^2} \sum_{k=1}^K \beta_k^2 (\mathbf{w}^H \hat{\mathbf{h}}_k) \mathbf{s}_k \mathbf{s}_k^H (\hat{\mathbf{h}}_k^H \mathbf{w}) \right). \quad (8)$$

Due to the determinant operator $\det(\cdot)$ and the $\mathbf{s}_k \mathbf{s}_k^H$ term, maximizing the above sum-rate expression is not an easy task. To manage that, we drop the spreading, and optimize the system as if no spreading is employed, i.e., we set $L = 1$ and $\mathbf{s}_k = 1, \forall k$. Such an optimization would correspond to a pure power-domain NOMA system, i.e., a worst-case scenario in which the spreading has no impact. Then, (8) becomes

$$R_{\text{sum}}^{(\text{no spread.})} = \log_2 \left(1 + \frac{1}{\sigma_{\tilde{\mathbf{n}}}^2} \sum_{k=1}^K \beta_k^2 \mathbf{w}^H \hat{\mathbf{h}}_k \hat{\mathbf{h}}_k^H \mathbf{w} \right). \quad (9)$$

Let $\mathbf{H} = \sum_{k=1}^K \beta_k^2 \hat{\mathbf{h}}_k \hat{\mathbf{h}}_k^H$, the sum-rate maximizer is given by

$$\begin{aligned} \mathbf{w}_{\text{sum}} &= \arg \max_{\mathbf{w}} \mathbf{w}^H \mathbf{H} \mathbf{w} \\ \text{s.t. } & |[\mathbf{w}]_n| = 1, \quad n = 1, 2, \dots, N_s, \end{aligned} \quad (10)$$

where the condition $|[\mathbf{w}]_n| = 1$ refers to the n^{th} element of \mathbf{w} performing a phase-shift only. In order to solve (10), we relax it to a conventional quadratic problem. Therefore, the maximizer of $\mathbf{w}^H \mathbf{H} \mathbf{w}$ is given by the eigenvector of \mathbf{H} corresponding to its maximum eigenvalue. Let \mathbf{u}_{max} be that eigenvector, the elements of \mathbf{w}_{sum} are then set to

$$[\mathbf{w}_{\text{sum}}]_n = \exp(j\angle[\mathbf{u}_{\text{max}}]_n), \quad n = 1, 2, \dots, N_s, \quad (11)$$

i.e., \mathbf{w}_{sum} is set such that it performs the same phase-shifts as \mathbf{u}_{max} . The issue with the sum-rate optimized shifts is that if the UEs have similar receive powers, then the RIS would boost all of them by an equal amount, i.e., it only provides a signal-to-noise ratio (SNR) gain (the strongest eigenvector would point in the direction that favors all the UEs). This is beneficial if the system suffers from low SNR; however, our major problem here is multi-user interference, and the goal is to boost the UEs with different portions, such that sufficient power gaps are created between them, allowing the IC to operate successfully. Also, in our optimization above, spreading is not taken into account. However, if the UEs have sufficient power gaps between them (e.g., due to different pathlosses), then \mathbf{w}_{sum} can provide a good solution, as the strongest eigenvector would point in the direction of the strongest UEs, and this helps to further enlarge the gaps (the RIS would boost the stronger UEs further), resulting in better sequential SINRs under IC. We will see this effect later in Section V.

IV. PROPOSED OPTIMIZATION APPROACH

Robust optimization of the phase-shifts requires solving the inequalities of (7). However, as we mentioned before, the optimal solution is difficult to obtain, due to the coupling between the detection order and the MMSE filter with our \mathbf{w} . In the following, we propose a suboptimal procedure that allows us to obtain a solution to the problem.

A. Detection Order

The optimal solution requires an exhaustive search over all possible detection orders, consisting of $K!$ possibilities. This can be prohibitive for large K , and it is the large K that we are interested in. A suboptimal approach that can provide a good performance [7], is to order the UEs based on their received signal strength, i.e., $|\beta_k \mathbf{w}^H \hat{\mathbf{h}}_k|$. However, we can see that it depends on \mathbf{w} , which we seek to find in the first place. For that reason, we do the ordering based on the sum-rate optimized shifts, i.e., by ordering the UEs according to $|\beta_k \mathbf{w}_{\text{sum}}^H \hat{\mathbf{h}}_k|$. In other words, \mathbf{w}_{sum} is employed as the initial solution for determining the detection order. In the following, and without loss of generality, we assume the resultant UEs ordering is

$$|\beta_1 \mathbf{w}_{\text{sum}}^H \hat{\mathbf{h}}_1| \geq |\beta_2 \mathbf{w}_{\text{sum}}^H \hat{\mathbf{h}}_2| \geq \dots \geq |\beta_K \mathbf{w}_{\text{sum}}^H \hat{\mathbf{h}}_K|, \quad (12)$$

that is, after ordering, UE 1 is the strongest user, while UE K is the weakest one. This assumption is only applied to simplify notation for the next parts.

B. MMSE Filtering

The next coupled variable is the MMSE filter. We follow a similar approach as with the detection order. We calculate the MMSE filters based on the sum-rate solution. Therefore, given our determined detection order and \mathbf{w}_{sum} , the MMSE filters applied in (6) are such that

$$\mathbf{v}_k^H = \mathbf{g}_k^H \left(\sum_{l=k}^K \mathbf{g}_l \mathbf{g}_l^H + \mathbf{I}_L \sigma_n^2 \right)^{-1}, \quad (13)$$

where $\mathbf{g}_k = \beta_k (\mathbf{w}_{\text{sum}}^H \hat{\mathbf{h}}_k) \mathbf{s}_k$.

C. Phase-Shifts Optimization

Having both the detection order and MMSE filter determined based on \mathbf{w}_{sum} , we now proceed to finding our final phase-shifts. First, we rewrite (6) as

$$\frac{\mathbf{w}^H \left(\beta_k^2 |\mathbf{v}_k^H \mathbf{s}_k|^2 \hat{\mathbf{h}}_k \hat{\mathbf{h}}_k^H \right) \mathbf{w}}{\mathbf{w}^H \left(\sum_{l=k+1}^K \beta_l^2 |\mathbf{v}_l^H \mathbf{s}_l|^2 \hat{\mathbf{h}}_l \hat{\mathbf{h}}_l^H + \frac{\sigma_n^2 \|\mathbf{v}_k\|^2}{N_s} \mathbf{I}_{N_s} \right) \mathbf{w}}, \quad (14)$$

where the fact that $\mathbf{w}^H \mathbf{w} = N_s$ has been applied to the noise term. Let

$$\begin{aligned} \mathbf{A}_k &= \beta_k^2 |\mathbf{v}_k^H \mathbf{s}_k|^2 \hat{\mathbf{h}}_k \hat{\mathbf{h}}_k^H, \\ \mathbf{B}_k &= \sum_{l=k+1}^K \beta_l^2 |\mathbf{v}_l^H \mathbf{s}_l|^2 \hat{\mathbf{h}}_l \hat{\mathbf{h}}_l^H + \frac{\sigma_n^2 \|\mathbf{v}_k\|^2}{N_s} \mathbf{I}_{N_s}, \end{aligned} \quad (15)$$

our optimization problem is then formulated as

$$\begin{aligned} \text{find } & \mathbf{w} \\ \text{s.t. } & \frac{\mathbf{w}^H \mathbf{A}_k \mathbf{w}}{\mathbf{w}^H \mathbf{B}_k \mathbf{w}} \geq \epsilon_k, \quad k = 1, 2, \dots, K, \\ & |[\mathbf{w}]_n| = 1, \quad n = 1, 2, \dots, N_s. \end{aligned} \quad (16)$$

To find a solution to those series of inequalities, we relax (16) into a SDP problem, which can be solved efficiently using convex optimization algorithms [15]. Let $\mathbf{W} = \mathbf{w} \mathbf{w}^H$; using the trace operator, we have $\mathbf{w}^H \mathbf{A}_k \mathbf{w} = \text{tr}(\mathbf{A}_k \mathbf{w} \mathbf{w}^H) = \text{tr}(\mathbf{A}_k \mathbf{W})$. Similarly, we have $\mathbf{w}^H \mathbf{B}_k \mathbf{w} = \text{tr}(\mathbf{B}_k \mathbf{W})$. The SINR condition is then written as

$$\begin{aligned} \text{tr}(\mathbf{A}_k \mathbf{W}) - \epsilon_k \text{tr}(\mathbf{B}_k \mathbf{W}) &\geq 0, \\ \text{tr}([\mathbf{A}_k - \epsilon_k \mathbf{B}_k] \mathbf{W}) &\geq 0. \end{aligned} \quad (17)$$

Finally, our SDP-relaxed problem is given by

$$\begin{aligned} \text{find } & \mathbf{W} \\ \text{s.t. } & \text{tr}([\mathbf{A}_k - \epsilon_k \mathbf{B}_k] \mathbf{W}) \geq 0, \quad k = 1, 2, \dots, K, \\ & \mathbf{W} \succeq 0, [\mathbf{W}]_{n,n} = 1, \quad n = 1, 2, \dots, N_s, \end{aligned} \quad (18)$$

where $[\mathbf{W}]_{n,n}$ is the n^{th} diagonal element of \mathbf{W} . In this work, the optimizer used is based on CVX [16]. If a solution is found, then we set \mathbf{w}_{prop} (proposed) such that it performs the same phase-shifts as the eigenvector of \mathbf{W} corresponding to its maximum eigenvalue (best rank-1 approximation) in a similar fashion as in (11). If no solution is feasible, then we rely on the sum-rate solution, i.e., we set $\mathbf{w}_{\text{prop}} = \mathbf{w}_{\text{sum}}$.

V. INVESTIGATION OF AN EXAMPLE SCENARIO

We consider a scenario where K active UEs in the target cluster communicate with a 32-antennas BS through a 32-elements RIS. A 4×16 Grassmannian codebook is employed for the spreading, i.e., the signature length is $L = 4$ with a total of 16 signatures in the codebook. The Grassmannian criterion refers to designing the codebook such that the maximum cross-correlation between any pair of signatures is minimized [17]. The BS-RIS channel is LOS with pathloss $\ell_{BS} = -65$ dB, while the RIS-UE channels are modeled as Rayleigh fading with the pathloss uniformly disturbed as $\ell_{h_k} \sim \mathcal{U}(-65 - s, -65 + s)$ dB, i.e., a mean component of -65 dB plus a spread of $\pm s$. By adjusting s , we can control the pathloss differences across the UEs, and thus the average received power difference between the UEs at the BS. We assume the UEs to transmit with an equal power of $P_k = P = 30$ dBm, $\forall k$. The noise power is set to $\sigma_n^2 = -110$ dBm. Also, we assume all the UEs to have the same threshold $\epsilon_k = \epsilon$. The simulation points are given with 95% confidence intervals shown as gray bars.

In Figure 2, we compare the detection performance using our proposed approach versus the sum-rate optimized phase-shifts and random ones. The results are shown for a pathloss spread of ± 3 dB, and over the outage thresholds of $\epsilon = 1, 4$, and 9 dB. The desired result here is a 1:1 line, i.e., all active UEs are detected correctly. We observe that our proposed RIS adaptation allows for a substantial increase of the number of correctly detected users. This is achieved at both low and high outage thresholds. As the threshold increases, it becomes more challenging for the RIS to satisfy all the inequalities of (7). If the threshold is too high for the number of active UEs, then no feasible solution would be possible, and the number of correctly detected UEs begins to drop.

Next, we set $K = 12$ and $\epsilon = 4$ dB and investigate the performance over different pathloss spreads. We also compare our NOMA (Grassmannian) codebook to an orthogonal multiple access (OMA) codebook, e.g., a 4×4 identity matrix. In the case of the OMA codebook, we only have 4 signatures, and therefore unique signature assignment to the 12 UEs is not possible, i.e., the orthogonal signatures must be reused between the users. The results are shown in Figure 3. We observe that, at least for the considered configuration, the NOMA codebook offers substantial improvement over the OMA codebook reuse strategy, across the different adaptation approaches. The NOMA codebook distributes the interference across all the signatures, which leads to improved performance under IC, as canceling one UE would help in improving the SINR of all remaining UEs, and not just to a limited subset as would occur when reusing the OMA codebook. We see that our approach provides a robust adaptation of the RIS phase-shifts with respect to the pathloss spread, and is able to create the necessary power gaps that result in the required SINR levels. As for the sum-rate optimized phases, we observe that the performance improves as the pathloss spread increases. As explained in Section III, the power gap between the UEs resulting from the larger pathloss spreads goes in the favor

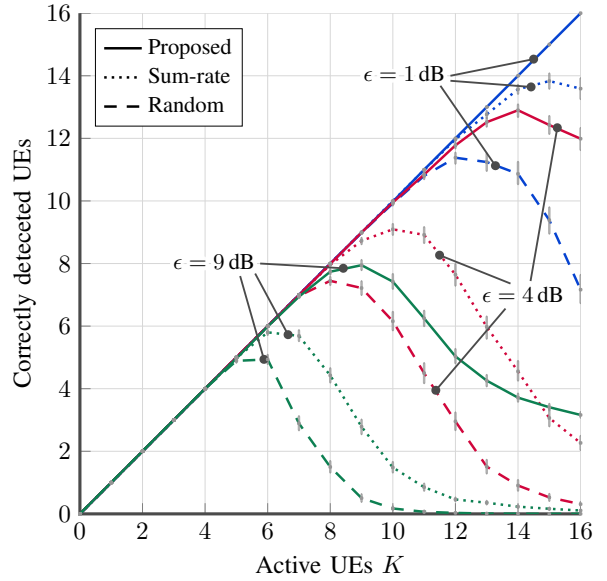


Fig. 2: Detectability under different strategies. Here $N_s = 32$, $P = 30$ dBm, and pathloss spread is ± 3 dB.

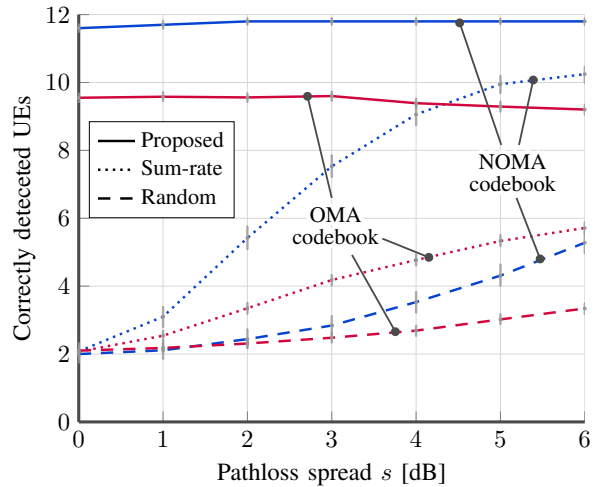


Fig. 3: Impact of the pathloss spread and codebook design on the performance. Here $N_s = 32$, $K = 12$, and $\epsilon = 4$ dB.

of the sum-rate solution. At low pathloss spreads, their user-separability performance approaches that of the random shifts. The gain at those ranges is mostly an SNR gain, which is not visible in the figure due to the relatively high transmit power.

To further investigate that, in Figure 4 we show the performance over the number of RIS elements N_s , for low and high transmit powers of $P = -5$ dBm and 30 dBm, respectively. We set the pathloss spread to ± 0 dB and $\epsilon = 3$ dB. First, we make the observation that a certain number of elements is required in order for (7) to be solvable; second, at low transmit powers and 0 dB pathloss spread, the sum-rate optimized phase-shifts clearly provide an SNR gain compared to the random phase-shifts, converging towards the performance of that at high transmit power as N_s increases. Our approach, as can be seen, is capable of providing both SNR and SINR gains under IC.

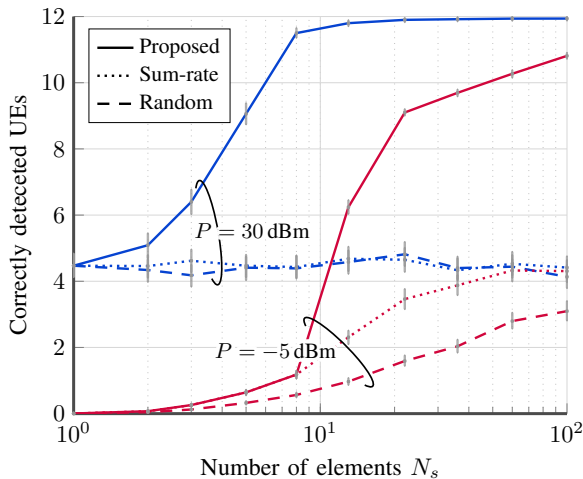


Fig. 4: Scaling of the performance with N_s . Here $K = 12$, $\epsilon = 3$ dB, and pathloss spread is ± 0 dB.

VI. DISCUSSION

We discuss in this section some aspects regarding our approach and assumptions, and possible further improvements.

- The spatial filtering applied is based on MRC, following the assumption of the BS being equipped with a large antenna array. If strong intercluster interference is present, then MMSE-based spatial filtering is a possibility. The model in (5) would still hold, except that an MMSE filter is applied instead of \mathbf{a}^H . Another solution, which is based on the code-domain, is to jointly design the spreading codebooks across the different clusters [18], such that the cross-correlation between the signatures of the neighbouring clusters is reduced.

- Throughout our optimization approach, we assumed the UEs to have fixed transmit powers. Power control can help improve the performance of the uplink, by adjusting the transmit power of UEs depending on their channel conditions. Therefore, further improvement of the performance can be achieved by jointly optimizing the RIS phase-shifts and the transmit powers.

- The assignment of the signatures to the UEs can also have an impact on the performance. In this work, we assumed a fixed signature assignment; still, we can utilize the structure of non-uniform codebooks such that UEs close in receive power are assigned near-orthogonal signatures, which then allows to suppress the interference between them by filtering. On the other hand, UEs with large power gaps can be assigned the same signature, since those can be separated via IC. However, this is also coupled with our phase-shifts optimization.

- Although we assumed the use of successive MMSE-IC detection, several alternatives are possible. For example, parallel IC can be performed, allowing multiple UEs to be detected per IC iteration, which reduces the detection latency for large K . Also, under certain conditions, the NOMA filtering can be performed in a low-complexity manner [19].

- For the extraction of the final phase-shifts in (18), a rank-1 approximation based on the strongest eigenvector was applied. In general, better approximation might be achieved via a Gaussian randomization procedure [15].

VII. CONCLUSION

We investigate the combination of code-domain NOMA and RISs in a massive MIMO cluster-based deployment. In order to support multi-user transmission within the clusters, code-domain NOMA is employed. We consider the optimization of the RIS such that a large number of users are detected correctly. To overcome the coupling between the RIS phase-shifts and other variables, such as the detection order and the applied filters, we utilize sum-rate optimized phase-shifts to obtain a decoupled estimate of those variables. Given the now-decoupled problem, the final phase-shifts are found by an SDP relaxation of the problem, which can be solved efficiently via convex optimization methods. Simulations results show that our approach is an effective RIS adaptation strategy.

REFERENCES

- [1] M. D. Renzo *et al.*, “Smart radio environments empowered by reconfigurable AI meta-surfaces: an idea whose time has come,” *EURASIP Journal on Wireless Communications and Networking*, vol. 2019, no. 1, p. 129, May 2019.
- [2] Q. Wu and R. Zhang, “Intelligent Reflecting Surface Enhanced Wireless Network via Joint Active and Passive Beamforming,” *IEEE Transactions on Wireless Communications*, vol. 18, no. 11, pp. 5394–5409, 2019.
- [3] —, “Towards Smart and Reconfigurable Environment: Intelligent Reflecting Surface Aided Wireless Network,” *IEEE Communications Magazine*, vol. 58, no. 1, pp. 106–112, 2020.
- [4] E. Basar *et al.*, “Wireless Communications Through Reconfigurable Intelligent Surfaces,” *IEEE Access*, vol. 7, pp. 116 753–116 773, 2019.
- [5] M. Fu, Y. Zhou, and Y. Shi, “Intelligent Reflecting Surface for Downlink Non-Orthogonal Multiple Access Networks,” in *2019 IEEE Globecom Workshops (GC Wkshps)*, 2019, pp. 1–6.
- [6] Z. Ding and H. Vincent Poor, “A Simple Design of IRS-NOMA Transmission,” *IEEE Communications Letters*, vol. 24, no. 5, pp. 1119–1123, 2020.
- [7] G. Yang, X. Xu, and Y. Liang, “Intelligent Reflecting Surface Assisted Non-Orthogonal Multiple Access,” in *2020 IEEE Wireless Communications and Networking Conference (WCNC)*, 2020, pp. 1–6.
- [8] X. Mu *et al.*, “Exploiting Intelligent Reflecting Surfaces in NOMA Networks: Joint Beamforming Optimization,” *IEEE Transactions on Wireless Communications*, vol. 19, no. 10, pp. 6884–6898, 2020.
- [9] A. S. d. Sena *et al.*, “What Role Do Intelligent Reflecting Surfaces Play in Multi-Antenna Non-Orthogonal Multiple Access?” *IEEE Wireless Communications*, vol. 27, no. 5, pp. 24–31, 2020.
- [10] L. Dai *et al.*, “A Survey of Non-Orthogonal Multiple Access for 5G,” *IEEE Communications Surveys Tutorials*, vol. 20, no. 3, pp. 2294–2323, 2018.
- [11] Z. Ding *et al.*, “Application of Non-Orthogonal Multiple Access in LTE and 5G Networks,” *IEEE Communications Magazine*, vol. 55, no. 2, pp. 185–191, 2017.
- [12] Y. Cai *et al.*, “Modulation and Multiple Access for 5G Networks,” *IEEE Communications Surveys Tutorials*, vol. 20, no. 1, pp. 629–646, 2018.
- [13] Z. Wu *et al.*, “Comprehensive Study and Comparison on 5G NOMA Schemes,” *IEEE Access*, vol. 6, pp. 18 511–18 519, 2018.
- [14] D. Tse and P. Viswanath, *Fundamentals of Wireless Communication*. Cambridge University Press, 2005.
- [15] Z. Luo *et al.*, “Semidefinite Relaxation of Quadratic Optimization Problems,” *IEEE Signal Processing Magazine*, vol. 27, no. 3, pp. 20–34, 2010.
- [16] M. Grant and S. Boyd, “CVX: Matlab Software for Disciplined Convex Programming, version 2.1,” <http://cvxr.com/cvx>, Mar. 2014.
- [17] B. Tahir, S. Schwarz, and M. Rupp, “Constructing Grassmannian Frames by an Iterative Collision-Based Packing,” *IEEE Signal Processing Letters*, vol. 26, no. 7, pp. 1056–1060, 2019.
- [18] —, “Joint Codebook Design for Multi-Cell NOMA,” in *ICASSP 2019 - 2019 IEEE International Conference on Acoustics, Speech and Signal Processing (ICASSP)*, 2019, pp. 4814–4818.
- [19] —, “Low-Complexity Detection of Uplink NOMA by Exploiting Properties of the Propagation Channel,” in *ICC 2020 - 2020 IEEE International Conference on Communications (ICC)*, 2020, pp. 1–6.